

# Near-Contact Motion of Surfactant-Covered Spherical Drops: Ionic Surfactant

Jerzy Bławdziewicz,<sup>1</sup> Vittorio Cristini, and Michael Loewenberg<sup>2</sup>

*Department of Chemical Engineering, Yale University, New Haven, Connecticut 06520–8286*

Received July 27, 1998; accepted November 18, 1998

**A lubrication analysis is presented for near-contact axisymmetric motion of spherical drops covered with an insoluble nondiffusing surfactant. The surfactant equation of state is arbitrary; detailed results are presented for ionic surfactants. The qualitative behavior of the system is determined by the dimensionless force parameter  $\hat{F}$ , the external force normalized by the maximum resistance force generated by Marangoni stresses. For  $\hat{F} > 1$  drops coalesce on a time scale commensurate with the coalescence time  $\tau_0$  for drops with clean interfaces. For  $\hat{F} < 1$ , the system evolves on the time scale  $\tau_0$  until Marangoni stresses approximately balance the external force; thereafter a slow evolution occurs on the Stokes time scale. In the long-time regime a self-similar surfactant concentration profile is attained that scales with the extent of the near-contact region. The gap width decreases exponentially with time but slower than for rigid particles because of surfactant backflow. For  $\hat{F} < 1$ , drop coalescence does not occur without van der Waals attraction. Quantitative results depend only moderately on the surfactant equation of state.** © 1999 Academic Press

**Key Words:** drop coalescence; surfactant; interfacial mobility; lubrication.

## 1. INTRODUCTION

Adsorbed surfactant affects hydrodynamic interactions between emulsion drops and modifies the short-range attractive and repulsive forces that act between drop interfaces (1). Either mechanism may help to stabilize emulsion drops against coalescence. Here, we focus on the hydrodynamic interactions between surfactant-covered drops.

In the absence of van der Waals attraction, rigid spherical particles are stable against aggregation because of the large pressure required to expel fluid from the narrow gap between rigid surfaces. By contrast, spherical drops with surfactant-free fully mobile interfaces coalesce readily because fluid can be more easily squeezed out of the near-contact region (2). Marangoni stresses (surface tension gradients) arising from gradients of surfactant concentration affect

hydrodynamic interactions (3). Marangoni stresses in the near-contact region between surfactant-covered drops oppose the lubrication flow out of the gap and thus hinder their approach.

Drops remain spherical provided that capillary stresses dominate deforming viscous stresses. Under these conditions surface tension gradients often maintain a nearly uniform surfactant distribution; thus, the surfactant is incompressible. Hydrodynamic interactions between spherical drops covered with insoluble incompressible surfactant have recently been analyzed (4). The results show that surfactant-covered drops generally behave differently than rigid spherical particles or drops with clean interfaces. However, in axisymmetric motion drops covered with nondiffusing incompressible surfactant behave like rigid spheres.

Surfactant compressibility is important for small concentrations of adsorbed surfactant. The recent lubrication analysis (5) for near-contact motion of drops covered with insoluble compressible surfactant reveals a complex nonlinear behavior. Under these conditions the system evolves on two time scales: a short time scale commensurate with the coalescence time for drops with clean interfaces and a long time scale characteristic of rigid spheres. The critical force for drop coalescence in the absence of van der Waals attraction was determined. The linear ideal gas equation of state was used to describe surface tension, which is often appropriate for low surfactant concentrations.

Nonlinear equations of state, however, are appropriate even for low surfactant concentrations if there are long-range interactions (e.g., Coulombic interactions) between surfactant molecules. In this paper, we generalize our earlier analysis (5) to an arbitrary equation of state. As a specific example, we consider an equation of state for ionic surfactants (6).

The assumptions of our analysis are stated in Section 2. The equations that describe the relative drop motion and the evolution of surfactant on the drop surfaces are given in Section 3. In Section 4, we discuss the two-time-scale behavior of the system. The short- and long-time regimes are analyzed in Sections 5 and 6. Concluding remarks are made in Section 7.

<sup>1</sup> Permanent address: IPPT PAN, Świętokrzyska 21, 00-049 Warsaw, Poland.

<sup>2</sup> To whom correspondence should be addressed.

## 2. ASSUMPTIONS

### 2.1. Insoluble Nondiffusing Surfactant

A lubrication analysis is used to describe axisymmetric near-contact approach of two surfactant-covered spherical drops. The drops have radii  $a_1$  and  $a_2$ , and are separated by a gap width  $h_0 \ll a$ , where  $a = (a_1^{-1} + a_2^{-1})^{-1}$  is the reduced radius. The extent of the near-contact region scales with  $\sqrt{ah_0}$ . The continuous-phase fluid has viscosity  $\mu$ , and the drops have viscosity  $\lambda\mu$ . The drops move with relative velocity  $U$  under the action of constant equal and opposite external forces that have magnitude  $F$ .

On the interface, the local surfactant concentration is  $\Gamma$ , and  $\Gamma = \Gamma_0$  at the edge of the near-contact region. Surfactant is characterized by an equation of state

$$\sigma(\Gamma) - \sigma(0) = -\beta(\Gamma), \quad [2.1]$$

where  $\sigma(\Gamma)$  is interfacial tension. Thermodynamic stability requires

$$\frac{d\beta}{d\Gamma} > 0. \quad [2.2]$$

The surfactant is assumed to be insoluble and nondiffusing. Surfactant solubility is unimportant for

$$\frac{\Gamma_0}{c_B} \gg h_0, \quad [2.3]$$

and surfactant diffusion is unimportant for (4)

$$\frac{\mu M_s}{\Gamma_0 h_0} \ll 1, \quad [2.4]$$

where  $c_B$  is the bulk equilibrium concentration of surfactant, and  $M_s$  is the collective surface mobility of the surfactant molecules.

### 2.2. Surfactant Compressibility

Marangoni stresses resulting from the gradients of surfactant concentration induce flow and pressure fields in the near-contact region. The pressure gives rise to a resistance force  $F_M \sim \Delta\sigma a$  that opposes drop approach, where  $\Delta\sigma$  is the variation of surface tension within the near-contact region. A straightforward generalization of our earlier analysis (5) gives

$$F_M \leq F_s, \quad [2.5]$$

where

$$F_s = 4\pi\beta_0 a, \quad [2.6]$$

and  $\beta_0 = \beta(\Gamma_0)$ . The magnitude of surfactant redistribution is characterized by the dimensionless force parameter

$$\hat{F} = \frac{F}{F_s}. \quad [2.7]$$

Herein, we focus on the regime

$$\hat{F} = O(1), \quad [2.8]$$

in which the surfactant is compressible

$$\frac{\Delta\Gamma}{\Gamma_0} = O(1), \quad [2.9]$$

where  $\Delta\Gamma$  is the variation of surfactant concentration in the near-contact region.

Drop deformation is neglected in our analysis, which requires that the lubrication pressure  $p \sim F/ah_0$  in the near-contact region is dominated by the capillary pressure  $\sigma_0/a$ , where  $\sigma_0 = \sigma(\Gamma_0)$ . Accordingly, small-capillary-number conditions,

$$Ca = \frac{F}{\sigma_0 h_0} \ll 1, \quad [2.10]$$

are assumed.

Conditions [2.8] and [2.10] indicate that

$$\frac{\beta_0 a}{\sigma_0 h_0} \ll 1 \quad [2.11]$$

is required if surfactant compressibility is finite and drop deformation can be neglected. Thus, low concentrations of adsorbed surfactant are assumed.

For low surfactant concentrations, surface viscosity is unimportant and is therefore neglected. In the absence of long-range intermolecular forces, the ideal gas surfactant equation of state,

$$\beta(\Gamma) = kT\Gamma, \quad [2.12]$$

applies, where  $T$  is temperature and  $k$  is Boltzmann's constant. For ionic surfactants, however, a nonlinear equation of state is often required even for small surfactant concentrations, because of long-range Coulombic interactions between the surfactant molecules.

### 2.3. Ionic Surfactants

The simplest approach for calculating the surface tension of an interface covered with ionic surfactant is the mean-field description based on the Gouy–Chapman approximation of the electric double layer (7, 8). More detailed calculations require incorporation of the molecular structure of the ionic solution (9–11) and the surfactant. In our numerical calculations, we use the mean-field approximation.

Accordingly, the equation of state for low concentrations of adsorbed ionic surfactant in a symmetric electrolyte (i.e., co- and counterions with charge valence  $\pm z$ ) is (6)

$$\beta = kT\Gamma \left[ 1 + \frac{2\nu}{Z\bar{\Gamma}} (\sqrt{(Z\bar{\Gamma})^2 + 1} - 1) \right], \quad [2.13]$$

where

$$\bar{\Gamma} = \Gamma/\Gamma_0 \quad [2.14]$$

is the dimensionless surfactant concentration. The surface potential parameter is

$$Z = \frac{e^2 z_s \Gamma_0}{2\epsilon \kappa kT}, \quad [2.15]$$

where  $e$  is an electron charge,  $\kappa^{-1}$  is the Debye screening length, and  $\epsilon$  is the dielectric constant of the electrolyte. The charge valence of the surfactant molecules is  $z_s$ , and

$$\nu = z_s/z \quad [2.16]$$

is the valence ratio. For small values of the surface potential parameter,  $Z$  is equal to the  $\zeta$  potential normalized by  $2kT/ez$ ;  $Z = 1$  corresponds to  $\zeta \approx 50$  mV in a monovalent electrolyte at room temperature.

The ideal gas equation of state [2.12] is recovered for  $Z \ll 1$ . A second linear regime is obtained for  $Z \gg 1$ :

$$\beta = kT\Gamma(1 + 2\nu). \quad [2.17]$$

The limiting results [2.12] and [2.17] also hold for asymmetric electrolytes, provided that  $\nu$  in [2.17] is based on the counterion valence.

Electrostatic repulsion and van der Waals attraction are neglected on the assumptions that

$$h_0 \gg \kappa^{-1} \quad [2.18]$$

and

$$h_0 \gg h_A, \quad [2.19]$$

where

$$h_A = \left( \frac{Aa}{6F} \right)^{1/2} \quad [2.20]$$

is the range of van der Waals attraction obtained by equating the external and (unretarded) van der Waals forces and  $A$  is the Hamaker constant.

### 3. LUBRICATION EQUATIONS

In our earlier analysis (5), we derived lubrication equations describing the near-contact motion of surfactant-covered spherical drops; the surfactant was characterized by the linear equation of state [2.12]. In this section, we generalize the description to surfactants that are described by an arbitrary equation of state.

The profile of the near-contact region between spherical drops is

$$h = h_0 + \frac{x^2}{2a}, \quad [3.1]$$

where

$$\epsilon = \frac{h_0}{a} \ll 1 \quad [3.2]$$

is the dimensionless gap width, and  $x$  is the radial coordinate measured from the center of the lubrication region. We introduce the dimensionless radial coordinate

$$y = 1 - \frac{h_0}{h}, \quad [3.3]$$

which maps the near-contact region into the finite interval  $0 \leq y \leq 1$ .

We define the dimensionless velocity and time,

$$\bar{U} = \frac{U}{U_p}, \quad \bar{t} = \frac{t}{\tau_p}, \quad [3.4]$$

where

$$U_p = \frac{F\epsilon}{6\pi\mu a} \quad [3.5]$$

is the relative velocity for near-contact motion of rigid spheres, and

$$\tau_p = \frac{6\pi\mu a^2}{F} \quad [3.6] \quad -\frac{1}{\bar{U}} \frac{\partial \bar{\Gamma}}{\partial \bar{t}} = y(1-y) \frac{\partial \bar{\Gamma}}{\partial y} + (1-y)^2$$

is the associated time scale (i.e., Stokes time). The dimensionless equation of state is

$$\bar{\beta}(\bar{\Gamma}) = \frac{\beta(\Gamma)}{\beta_0}. \quad [3.7]$$

Generalized evolution equations that describe near-contact motion of surfactant-covered drops are obtained by replacing  $kT\Gamma$  with  $\beta(\Gamma)$  in the equations given in Section 3.1 of Ref. (5), and transforming the results to the dimensionless variables defined above. (Note the symbol change for surfactant concentration.) Accordingly, we have the kinematic condition

$$\frac{1}{\epsilon} \frac{d\epsilon}{dt} = -\bar{U} \quad [3.8]$$

and the equation of motion

$$\epsilon f \bar{U} = 1 - \frac{\hat{F}_M}{\hat{F}}, \quad [3.9]$$

where the external force  $\hat{F}$  and the Marangoni force  $\hat{F}_M$  are normalized by [2.6]. Equation [3.9] describes the balance between the external force, the lubrication resistance between drops with clean interfaces  $6\pi\mu a U f$ , and the Marangoni force

$$\hat{F}_M = \int_0^1 (1 - \bar{\beta}) dy, \quad [3.10]$$

which depends only on the instantaneous distribution of surfactant. According to (12)

$$f = \frac{\sqrt{2}\pi^2}{16} \epsilon^{-1/2} \lambda, \quad [3.11]$$

which holds for  $\epsilon^{1/2} \ll \lambda \ll \epsilon^{-1/2}$ , as assumed herein.

The distribution of insoluble nondiffusing surfactant evolves by convection with interfacial velocity

$$\frac{u}{U} = \sqrt{\frac{y(1-y)}{2\epsilon}} \left( 1 - \frac{1}{2\hat{F}\bar{U}} \frac{\partial \bar{\beta}}{\partial y} \right). \quad [3.12]$$

The surfactant equation of motion is

$$\times \left[ \frac{\partial(\bar{\Gamma}y)}{\partial y} - \frac{1}{2\hat{F}\bar{U}} \frac{\partial}{\partial y} \left( \bar{\Gamma}y \frac{\partial \bar{\beta}}{\partial y} \right) \right], \quad [3.13]$$

where

$$\bar{\Gamma} = 1 \quad \text{at } y = 1. \quad [3.14]$$

Boundary condition  $\partial \bar{\Gamma} / \partial x = 0$  is automatically enforced at  $x = 0$ , provided that  $\partial \bar{\Gamma} / \partial y$  is nonsingular at  $y = 0$ . Given the initial gap width  $\epsilon_0$  and the initial distribution of surfactant, [3.8]–[3.14] form a closed set of equations that describe the near-contact motion of surfactant-covered drops with accuracy  $O(\epsilon^{1/2})$ .

## 4. TWO-TIME-SCALE BEHAVIOR

### 4.1. Short- and Long-Time Regimes

An analysis of [3.8]–[3.14] indicates that two regimes associated with two time scales can be distinguished, depending on the balance between the external and the Marangoni forces.

The short-time regime is characterized by convection of surfactant from the near-contact region. Marangoni stresses develop, but the Marangoni force is too weak to balance the external force:

$$|\hat{F} - \hat{F}_M| \gg O(\epsilon^{1/2}). \quad [4.1]$$

Thus,

$$\frac{U}{U_0} = O(1), \quad [4.2]$$

according to [3.9], where

$$U_0 = \frac{F}{6\pi\mu a f} \gg U_p \quad [4.3]$$

is the relative velocity between drops with clean interfaces. The system evolves on a time scale commensurate with the coalescence time for drops with clean interfaces

$$\tau_0 = \frac{3}{4} \sqrt{2} \pi^3 \frac{\epsilon_0^{1/2} a^2 \mu \lambda}{F}, \quad [4.4]$$

where  $\tau_0 \ll \tau_p$ . The viscosity ratio sets the time scale but is otherwise unimportant. For a uniform initial distribution of surfactant,  $\hat{F}_M = 0$  at  $\bar{t} = 0$ ; thus, [4.1] applies.

In the complementary long-time regime, surfactant is no

longer convected from the near-contact region. The Marangoni force approximately balances the external force,

$$|\hat{F} - \hat{F}_M| = O(\epsilon^{1/2}), \quad [4.5]$$

and the relative velocity is comparable to that for rigid spheres,

$$\frac{U}{U_p} = O(1), \quad [4.6]$$

according to Eq. [A.6]. Thus, the system evolves on the rigid-particle time scale [3.6]. The viscosity ratio is unimportant in the long-time regime.

#### 4.2. Critical Force

Equations [2.2] and [3.10] indicate that  $\hat{F}_M \leq 1$ . Thus, external forces  $\hat{F} > 1$  cannot be balanced by the Marangoni force. Under these conditions, the entire evolution occurs in the short-time regime, and the drops coalesce.

For  $\hat{F} < 1$ , the Marangoni force increases until the long-time force balance [4.5] is established, and the relative velocity decreases. In the absence of van der Waals attraction, drops do not coalesce, according to [3.8] and [4.6].

We conclude that

$$\hat{F} = 1 \quad [4.7]$$

is the critical value of the force parameter for coalescence in the absence of van der Waals attraction. The effect of van der Waals forces is discussed in Section 5.3.

#### 4.3. Evolution of Gap Width and Marangoni Force

The two-time-scale behavior is illustrated in Fig. 1, where the evolution of gap width and Marangoni force is depicted for ionic and nonionic surfactants. The results demonstrate that for subcritical values of the force parameter the system evolves on the short-time scale until the force balance [4.5] is established. For supercritical values of the force parameter, drop coalescence occurs on the short-time scale.

The values of  $Z$  and  $\nu$  used for the calculations were selected to emphasize the effect of surfactant charge. In scaled variables, the qualitative behavior is unaffected by the values for  $Z$  and  $\nu$ , and the quantitative results are only moderately influenced.

Simplified descriptions for the short- and long-time regimes are formulated below.

### 5. SHORT-TIME BEHAVIOR

#### 5.1. Evolution of Surfactant Distribution

According to [4.2],  $\bar{U} = O(\epsilon^{-1/2})$ ; thus, terms arising from Marangoni stresses in [3.12] and [3.13] are small. At leading

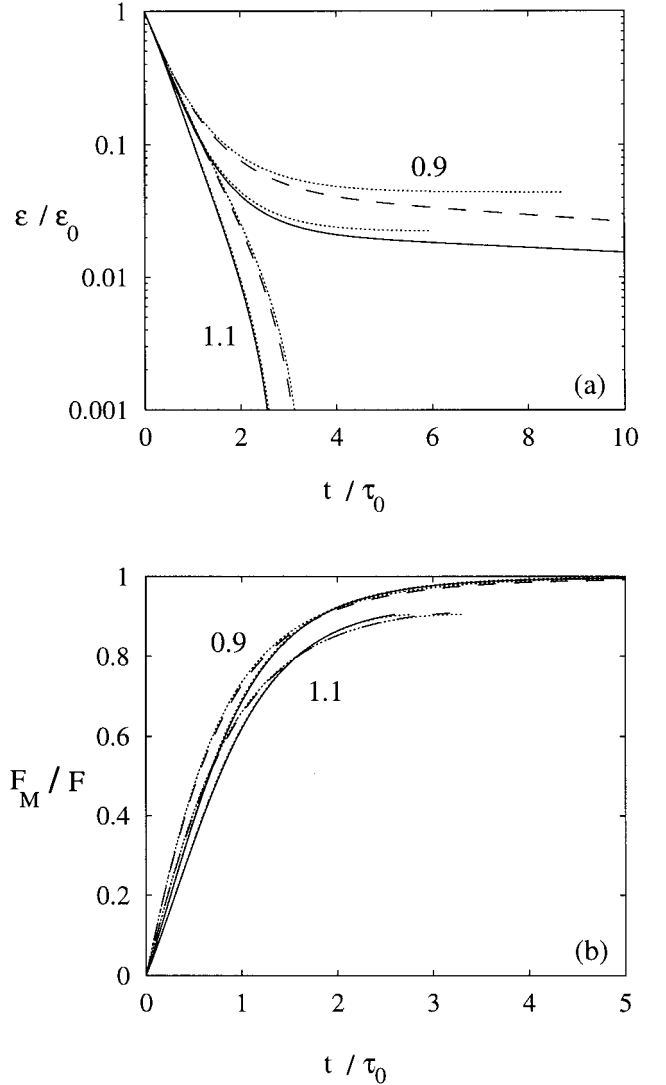


**FIG. 1.** Evolution of gap width (a) and Marangoni force (b) as functions of dimensionless time (normalized by the short time scale  $\tau_0$ ), for two values of  $\hat{F}$  (as labeled):  $\epsilon_0 = 0.01$ ,  $\lambda = 1$ , uniform initial distribution of surfactant:  $Z = 0, \infty$  (solid curves),  $Z = 1$ ,  $\nu = 3$  (dashed curves). Corresponding short-time solutions (dotted curves). Short-time and exact solutions nearly coincide, except for  $\hat{F} = 0.9$  in (a).

order, the normalized interfacial velocity  $u/U$  is the same as for drops with clean interfaces. Equation [3.13] reduces to a first-order linear equation with the solution (5)

$$\bar{\Gamma}_s = q(y)g(y'), \quad [5.1]$$

where  $g(y)$  is an arbitrary initial distribution of surfactant,

$$q = [1 + (\bar{\epsilon}^{-2} - 1)(1 - y)^2]^{-1/2}, \quad [5.2]$$

with  $\bar{\epsilon} = \epsilon/\epsilon_0$ , and

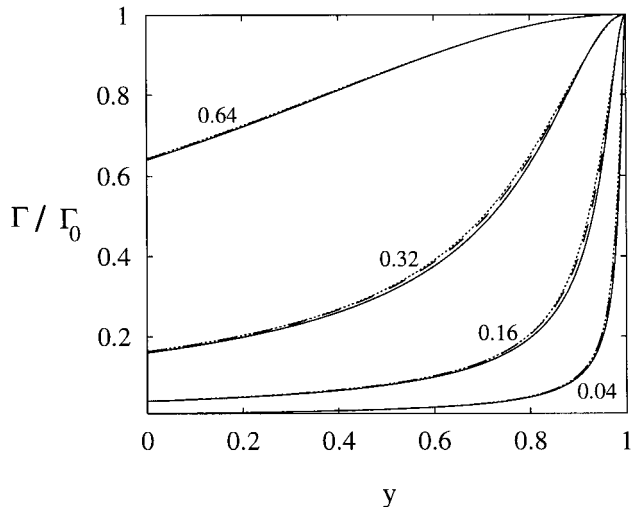


**FIG. 2.** Surfactant concentration profiles at different gap widths  $\bar{\epsilon}$  (as labeled),  $\hat{F} = 1.1$ ,  $\epsilon_0 = 0.01$ ,  $\lambda = 1$ , uniform initial distribution of surfactant:  $Z = 0, \infty$  (solid curves),  $Z = 1, \nu = 3$  (dashed curves). Corresponding short-time approximation (dotted curves).

$$y' = 1 - (1 - y)q(y) \tag{5.3}$$

is the convected coordinate. The result indicates that the surfactant distribution broadens continuously on the length scale of the lubrication region; at contact, surfactant is completely displaced from the lubrication region.

In Fig. 2, surfactant concentration profiles predicted by [5.1] are compared with numerical solutions of [3.8]–[3.14]. The results indicate that for  $\hat{F} > 1$  the short-time solution provides an accurate approximation for the entire evolution, even for near-critical values of the force parameter. (Greater accuracy is obtained for larger  $\hat{F}$ .)

5.2. Evolution of Gap Width and Marangoni Force

The short-time surfactant distribution [5.1] is independent of the surfactant equation of state. Surfactant is passively convected. However, surfactant concentration gradients produce the Marangoni force and therefore affect the gap width evolution.

The short-time approximation of the Marangoni force is obtained by inserting [5.1] into [3.10]:

$$\hat{F}_{MS}(\bar{\epsilon}) = \int_0^1 [1 - \bar{\beta}(\bar{\Gamma}_s)] dy. \tag{5.4}$$

The result is independent of the external force. The short-time near-contact velocity of the drops is obtained by inserting  $\hat{F}_M = \hat{F}_{MS}$  into [3.9]. On integration, [3.8] yields the short-time gap width evolution:

$$t(\bar{\epsilon}) = \tau_0 \int_{\bar{\epsilon}}^1 \frac{\hat{F}}{\hat{F} - \hat{F}_{MS}(s)} d\sqrt{s}. \tag{5.5}$$

The dotted curves shown in Fig. 1 represent the short-time solution [5.4] and [5.5].

For supercritical values of the force parameter, the short-time solution describes the entire evolution, as seen in Fig. 1. The coalescence time is accurately approximated by

$$\tau = t(0), \tag{5.6}$$

where  $t(\bar{\epsilon})$  is given by [5.5]. The formula indicates that the normalized coalescence time  $\tau/\tau_0$  is independent of the initial gap and the viscosity ratio. The drop coalescence time [5.6] is shown in Fig. 3 as a function of the force parameter for ionic and nonionic surfactants. The results indicate that the normalized drop coalescence time is only weakly affected by the surfactant equation of state.

For subcritical  $\hat{F}$ , the results depicted in Fig. 1 illustrate that the short-time solution describes the evolution until the force balance [4.5] is achieved. The short-time solution [5.5] stabilizes at a finite gap width  $\bar{\epsilon}_s$  that satisfies the balance

$$\hat{F}_{MS}(\bar{\epsilon}_s) = \hat{F}. \tag{5.7}$$

The stable gap width  $\epsilon_s$  is shown in Fig. 4 as a function of the force parameter for ionic and nonionic surfactants. The transition between the short-time [4.1] and long-time [4.5] regimes occurs at  $\epsilon \approx \epsilon_s$ . In the long-time regime, gap drainage continues on the Stokes time scale  $\tau_p$ , as discussed in Section 6.

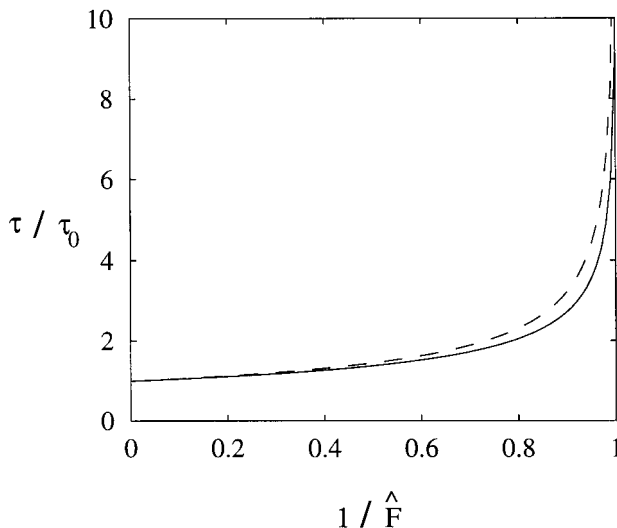


**FIG. 3.** Short-time solution for dimensionless drop coalescence time versus  $1/\hat{F}$ , uniform initial distribution of surfactant:  $Z = 0, \infty$  (solid curve);  $Z = 1, \nu = 3$  (dashed curve).

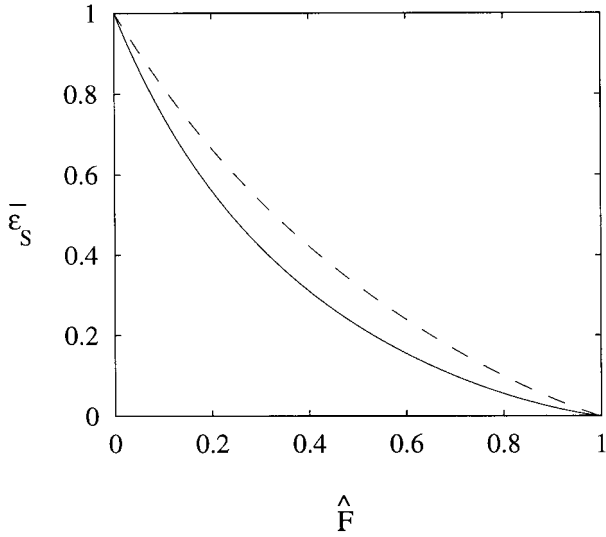


**FIG. 4.** Stable gap width defined by [5.7] versus force parameter, uniform initial distribution of surfactant:  $Z = 0, \infty$  (solid curve);  $Z = 1, \nu = 3$  (dashed curve).

### 5.3. Van der Waals Attraction

In the presence of van der Waals attraction, rapid coalescence occurs (unless repulsive forces are important) if  $\bar{\epsilon}_A > \bar{\epsilon}_s$ , where

$$\bar{\epsilon}_A = \frac{h_A}{\epsilon_0 a} \quad [5.8]$$

and  $h_A$  is the range of van der Waals attraction given by [2.20]. From [5.7] and [5.8], we obtain an equation for the critical value of the force parameter for rapid coalescence in the presence of van der Waals attraction:

$$\hat{F} \approx \hat{F}_{MS}(\bar{\epsilon}_A). \quad [5.9]$$

Drops are stable against rapid coalescence (on the time scale  $\tau_0$ ) for  $\hat{F} < \hat{F}_{MS}(\bar{\epsilon}_A)$ .

## 6. LONG-TIME BEHAVIOR

### 6.1. Surfactant Concentration and Interfacial Velocity Profiles

The results shown in Fig. 1 illustrate that the long-time force balance [4.5] is achieved on the time scale  $\tau_0$  for subcritical values of the force parameter. Evolution of the corresponding surfactant concentration and interfacial velocity profiles is shown in Fig. 5. The results reveal a rapid initial evolution on the time scale  $\tau_0$  which is replaced, at long times, by a slow evolution on the time scale  $\tau_p$ . For  $\bar{t} \rightarrow \infty$  the surfactant concentration and interfacial velocity profiles tend to self-similar forms in the lubrication variables and thus sharpen with

decreasing gap width. Under the conditions corresponding to Fig. 5a, a surfactant-free clean spot forms in the lubrication region at long times.

The long-time narrowing of the surfactant distribution is associated with surfactant backflow: the interfacial velocity is negative except where  $\bar{\Gamma} = 0$ . In contrast, the interfacial velocity is outward and the surfactant distribution broadens continuously in the short-time regime (cf. Fig. 2).

### 6.2. Similarity Solution

Evolution in the long-time regime is described by a reduced set of equations. From [3.10] and [4.5], we obtain

$$\hat{F} = \int_0^1 (1 - \bar{\beta}) dy, \quad [6.1]$$

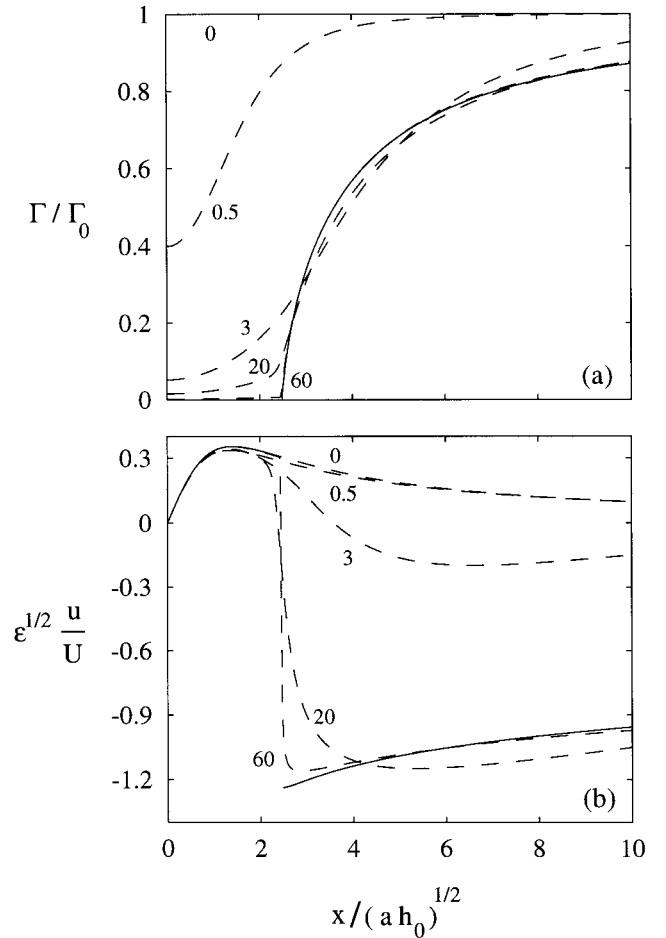


**FIG. 5.** Profiles of (a) surfactant concentration and (b) interfacial velocity at different dimensionless times  $t/\tau_0$  (as labeled) for drops pushed together with  $\hat{F} = 0.9$ ,  $Z = 1$ ,  $\nu = 3$ ,  $\lambda = 1$ ,  $\epsilon_0 = 0.01$  ( $\tau_p/\tau_0 = 5.73$ ), and uniform initial distribution of surfactant: numerical solution (dashed curves); long-time similarity solution (solid curves).

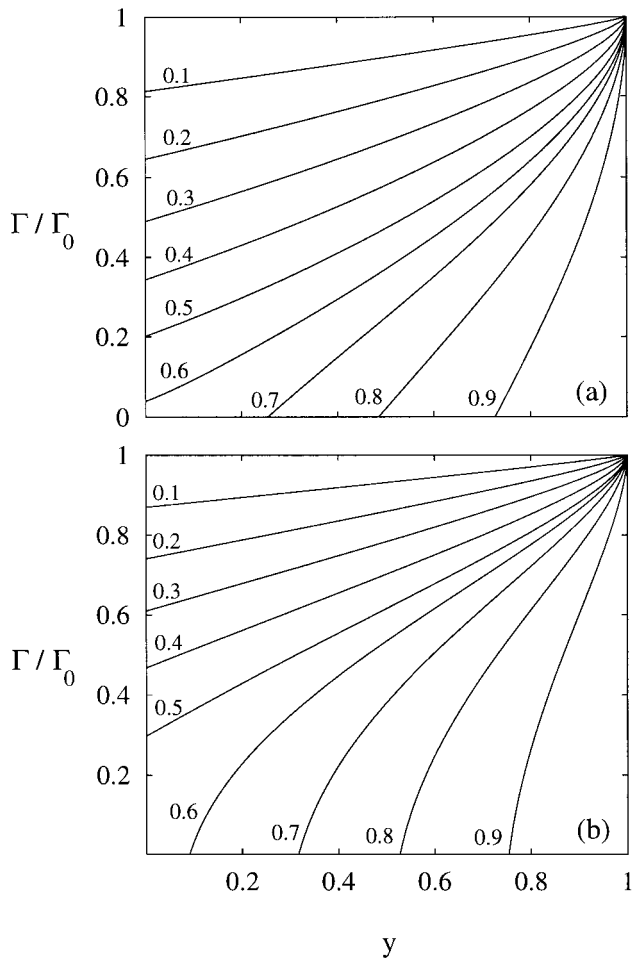


**FIG. 6.** Long-time similarity profiles of surfactant concentration for drops that are pushed together with different values of  $\hat{F}$  (as labeled):  $Z = 0, \infty$  (a);  $Z = 1, \nu = 3$  (b).

within the  $O(\epsilon^{1/2})$  accuracy of the full description [3.8]–[3.14]. Evolution of the surfactant distribution is governed by [3.13], with  $\bar{U}$  determined by the constraint [6.1], which yields [A.6]. The gap width is determined by the kinematic condition [3.8], but does not enter the evolution equations for the surfactant distribution. The long-time interfacial velocity profile is obtained from [3.12]. According to the foregoing description, the long-time evolution is independent of the viscosity ratio because Marangoni stresses dominate the hydrodynamic stresses resulting from circulation within the drops.

Stationary solutions of [3.13] yield concentration profiles that scale with the extent of the lubrication region and correspond to the  $\bar{t} \rightarrow \infty$  behavior illustrated in Fig. 5a. Under long-time stationary conditions, [3.13] reduces to an ordinary differential equation which is integrated according to the procedure described in Appendix B.

Long-time surfactant concentration profiles are depicted in Fig. 6. For sufficiently large subcritical values of the force parameter,  $1 > \hat{F} > \hat{F}_c$ , a surfactant-free clean spot forms.

The radius of the clean spot (for  $\hat{F} > \hat{F}_c$ ) and the surfactant concentration at  $x = 0$  (for  $\hat{F} < \hat{F}_c$ ) are shown in Fig. 7. For ionic surfactant described by [2.13], the onset of clean-spot formation corresponds to  $\hat{F} = \hat{F}_c$ , where  $0.56 \leq \hat{F}_c \leq 0.61$ , depending on the surface potential and charge valence parameters  $Z$  and  $\nu$ . For small and near-critical values of  $\hat{F}$ , analytical expressions for the long-time surfactant distribution are derived in Appendix B.

The dimensionless long-time relative velocity  $\bar{U}$  is constant and is obtained from the stationary surfactant distribution by the procedure described in Appendix B. According to Eq. [3.8], the gap width decreases exponentially, as seen in Fig. 1. At long times surfactant-covered drops thus behave qualitatively as rigid spheres.

The results shown in Fig. 8, however, indicate that  $\bar{U} \leq 1$  at long times: surfactant-covered drops have smaller relative velocities than rigid particles. An explanation follows from the long-time surfactant backflow, seen in Fig. 5b, which hinders flow from the near-contact region. As shown in Appendix B,

$$\bar{U} = 1 - \frac{2\hat{F}}{\beta'(1)}, \quad \hat{F} \ll 1, \quad [6.2]$$

and

$$\bar{U} = \frac{1}{2} \left[ 1 - \int_0^1 \bar{\beta}(\bar{\Gamma}) d\bar{\Gamma} \right], \quad \hat{F} = 1, \quad [6.3]$$

where  $\bar{\beta}' = d\bar{\beta}/d\bar{\Gamma}$ . In particular, rigid sphere behavior is recovered for  $\hat{F} \rightarrow 0$ , and

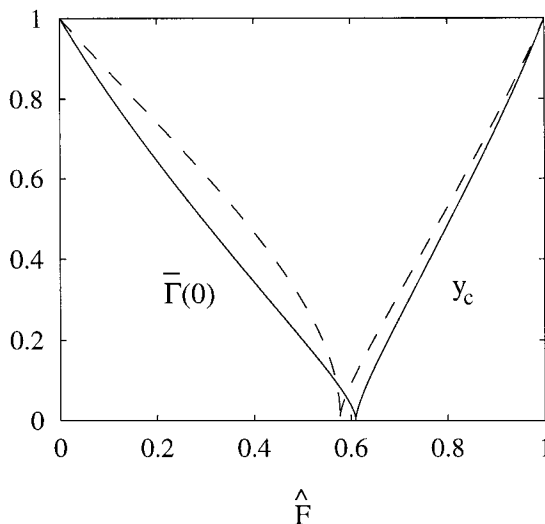


**FIG. 7.** Surfactant concentration at center of near-contact region  $\bar{\Gamma}(0)$  and radius of clean spot  $y_c$  at long times:  $Z = 0, \infty$  (solid curves);  $Z = 1, \nu = 3$  (dashed curves).

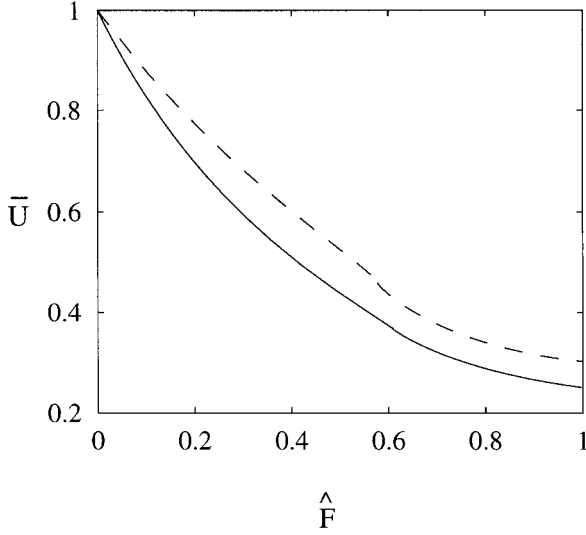


**FIG. 8.** Dimensionless long-time relative drop velocity:  $Z = 0, \infty$  (solid curve);  $Z = 1, \nu = 3$  (dashed curve).

$$\bar{U} < \frac{1}{2}, \quad \hat{F} = 1. \quad [6.4]$$

For ionic surfactant, characterized by [2.13], we have

$$\bar{\beta}'(1) = \frac{2\nu Z^2 + ZZ_1}{Z_1[Z + 2\nu(Z_1 - 1)]}, \quad [6.5]$$

$$\int_0^1 \bar{\beta}(\bar{\Gamma}) d\bar{\Gamma} = \frac{Z + 2\nu(Z_1 + Z^{-1} \sinh^{-1} Z - 2)}{2Z + 4\nu Z(Z_1 - 1)}, \quad [6.6]$$

where

$$Z_1 = (1 + Z^2)^{1/2}. \quad [6.7]$$

The limiting long-time velocity  $\bar{U}$  for  $\hat{F} = 1$ , as given by Eqs. [6.3] and [6.6], is shown in Fig. 9.

### 6.3. Response to External Force Fluctuations

We consider the response of the system in the long-time regime to an external force fluctuation  $\delta\hat{F}$ . Following the perturbation, surfactant redistributes on the short-time scale until the long-time force balance [4.5] is recovered. As shown in Appendix C, the associated gap width adjustment  $\delta\epsilon$  is described by

$$-\frac{1}{\epsilon} \frac{\delta\epsilon}{\delta\hat{F}} = \frac{1}{I_1}, \quad [6.8]$$

where  $I_1$  is given by [A.2].

If the long-time similarity solution is established prior to the force fluctuation,

$$-\frac{1}{\epsilon} \frac{\delta\epsilon}{\delta\hat{F}} = \frac{3}{\bar{\beta}'} + \frac{9\bar{\beta}''(1)}{2[\bar{\beta}'(1)]^3} \hat{F}, \quad \hat{F} \ll 1, \quad [6.9]$$

where  $\bar{\beta}'' = d^2\bar{\beta}/d\bar{\Gamma}^2$ , and

$$-\frac{1}{\epsilon} \frac{\delta\epsilon}{\delta\hat{F}} = \frac{1}{1 - \hat{F}}, \quad \hat{F} \rightarrow 1, \quad [6.10]$$

as shown in Appendix C. It follows that the stable gap width is most sensitive to fluctuations in the external force for near-critical  $\hat{F}$ .

For ionic surfactant characterized by Eq. [2.13],  $\bar{\beta}'(1)$  is given by [6.5] and

$$\bar{\beta}''(1) = \frac{2\nu Z^2}{Z_1^3[Z + 2\nu(Z_1 - 1)]}. \quad [6.11]$$

The sensitivity of gap width to external force fluctuations is illustrated in Fig. 10. The results indicate that for ionic surfactant near-contact motion is less sensitive to external force fluctuations.

## 7. CONCLUSIONS

A recently developed theory for the near-contact motion of surfactant-covered spherical drops (5) has been generalized to an arbitrary surfactant equation of state. Our earlier analysis was restricted to low concentrations of adsorbed surfactants that obey a linear equation of state. The neglect of drop

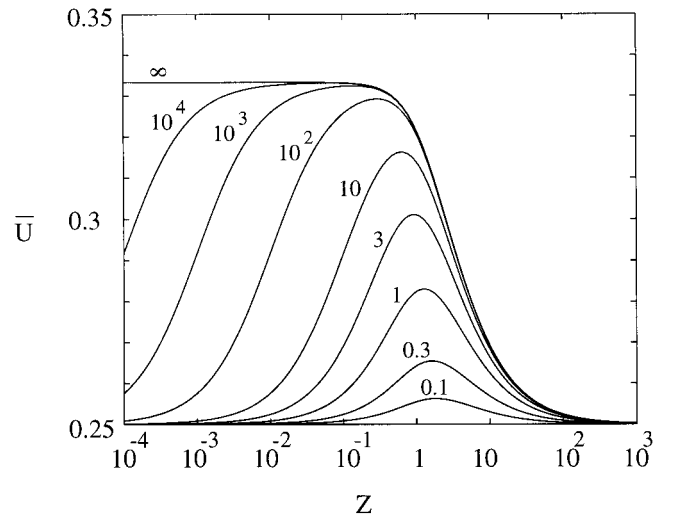


**FIG. 9.** Long-time limiting velocity  $\bar{U}$  for critical value of force parameter  $\hat{F} = 1$ , versus surface potential parameter  $Z$ , for different values of valence ratio  $\nu$  (as labeled).

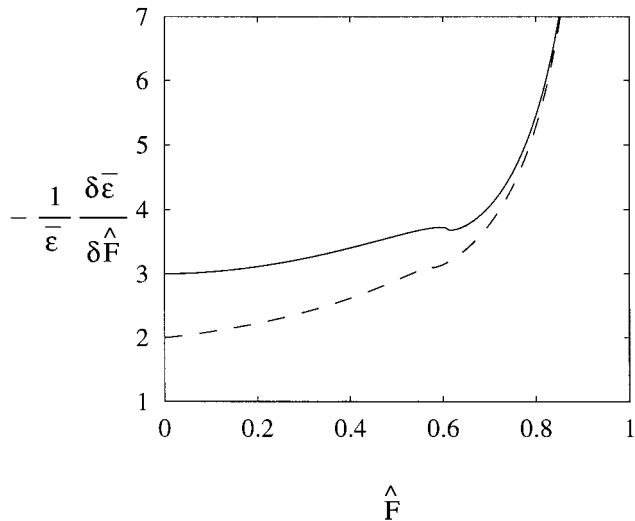


**FIG. 10.** Sensitivity of gap width to external force fluctuations versus  $\hat{F}$  in the long-time similarity regime, obtained from [6.8]:  $Z = 0, \infty$  (solid curve);  $Z = 1, \nu = 3$  (dashed curve).

deformation implies low surfactant concentrations; however, a nonlinear equation of state is required for ionic surfactants because of long-range Coulombic interactions between surfactant molecules.

Marangoni stresses hinder flow from the gap between approaching drops. The resulting resistance force has a maximal value  $F_s = 4\pi\beta(\Gamma_0)a$ , where  $\beta(\Gamma)$  is the surface tension reduction due to adsorbed surfactant. For an external pushing force  $F < F_s$ , the drops are stabilized against rapid coalescence.

The maximum Marangoni force  $F_s$  increases with the charge on the surfactant molecule. Thus, ionic surfactant can more effectively stabilize drops against coalescence (even if the electrostatic repulsion between the drop interfaces is unimportant). However, in a dimensionless formulation with characteristic force  $F_s$ , the results are qualitatively unaffected by the parameters  $Z$  and  $\nu$  that characterize the surfactant equation of state.

The evolution of surfactant-covered drops in near-contact motion occurs on two time scales. Initially, the system evolves on the short-time scale given by the coalescence time for drops with clean interfaces. Surfactant is convected from the near-contact region, and coalescence occurs for  $F > F_s$ .

At long times, the Marangoni and external forces approximately balance for  $F < F_s$ ; thereafter, the system evolves on the Stokes time. The surfactant distribution scales with the extent of the near-contact region and is independent of the initial conditions and internal-phase viscosity. For  $1 > F/F_s \gtrsim 0.6$ , a shrinking clean spot forms at the center of the near-contact region. The gap width decreases exponentially but more slowly than for rigid particles, because of the backflow of surfactant in the near-contact region. For  $F < F_s$ , coalescence relies on van der Waals attraction.

Criteria [2.4], [2.10], [2.18], and [2.19] are not uniformly valid for  $h_0 \rightarrow 0$ . At small gap widths surfactant diffusion, drop deformation, van der Waals attraction, and electrostatic repulsion become important. Future work should include an investigation of electrostatic interactions between interfaces with adsorbed ionic surfactant.

## APPENDIX A

### Short- and Long-Time Force Balance

The rate of change of the Marangoni force is found by multiplying both sides of [3.13] by  $\beta' = d\bar{\beta}/d\bar{\Gamma}$  and integrating with respect to  $y$ . Accordingly, we obtain

$$\frac{d\hat{F}_M}{dt} = I_1\bar{U} - \frac{I_2}{\hat{F}}, \quad [\text{A.1}]$$

where

$$I_1 = \int_0^1 \bar{\beta}'(\bar{\Gamma}) \left[ y(1-y) \frac{\partial \bar{\Gamma}}{\partial y} + (1-y)^2 \frac{\partial (y\bar{\Gamma})}{\partial y} \right] dy, \quad [\text{A.2}]$$

$$I_2 = \frac{1}{2} \int_0^1 \bar{\beta}'(\bar{\Gamma}) (1-y)^2 \frac{\partial}{\partial y} \left( y\bar{\Gamma} \bar{\beta}'(\bar{\Gamma}) \frac{\partial \bar{\Gamma}}{\partial y} \right) dy. \quad [\text{A.3}]$$

Here we assume that  $\partial \bar{\Gamma}/\partial y \geq 0$ , which is valid for approaching drops with a uniform initial surfactant distribution. Thus, by the thermodynamic stability condition [2.2],

$$I_1 > 0. \quad [\text{A.4}]$$

Equation [4.2] indicates that  $I_1\bar{U} \gg I_2/\hat{F}$  in the short-time regime. (The only exceptions occur for large initial variations of surfactant concentration.) Thus,

$$\frac{d}{dt} |\hat{F} - \hat{F}_M| < 0 \quad [\text{A.5}]$$

for constant  $\hat{F}$ , according to Eqs. [A.1] and [3.9]. The result indicates that the system evolves toward the stable long-time force balance [4.5], provided that  $\hat{F} < 1$ .

In the long-time regime,  $d\hat{F}_M/dt = 0$  for a constant external force; thus, the relative velocity of the drops is

$$\bar{U} = \frac{I_2}{I_1\hat{F}}, \quad [\text{A.6}]$$

according to Eq. [A.1].

## APPENDIX B

## Long-Time Similarity Solution

At long times, conservation equation [3.13] reduces to an ordinary differential equation that describes long-time self-similar surfactant distributions,

$$y \frac{d\bar{\Gamma}}{dy} + (1-y) \left[ \frac{d(\bar{\Gamma}y)}{dy} - \frac{1}{\gamma} \frac{d}{dy} \left( \bar{\Gamma}y \frac{d\bar{\beta}}{dy} \right) \right] = 0, \quad [\text{B.1}]$$

where

$$\gamma = 2\hat{F}\bar{U}. \quad [\text{B.2}]$$

Equation [B.1] was numerically integrated with initial condition

$$\bar{\Gamma} = \bar{\Gamma}_0 \quad \text{at } y = 0, \quad [\text{B.3}]$$

where  $\bar{\Gamma}_0 > 0$ , or

$$\bar{\Gamma} = 0 \quad \text{at } y = y_c, \quad [\text{B.4}]$$

where  $y_c > 0$  is the extent of the clean spot with  $\bar{\Gamma} = 0$ . Only one initial condition is needed because [B.1] reduces to a first-order differential equation for  $y \rightarrow 0$  or  $\bar{\Gamma} \rightarrow 0$ . Boundary condition [3.14] is used to determine  $\gamma$ , and the values for  $\hat{F}$  and  $\bar{U}$  are then obtained from Eq. [6.1]. Analytical solutions of [B.1]–[B.4] for small and near-critical values of the force parameter are derived below.

For  $\hat{F} \ll 1$  an expansion of Eq. [B.1] in  $\gamma$  yields

$$\bar{\Gamma} = 1 + \gamma\bar{\Gamma}_1 + \gamma^2\bar{\Gamma}_2 + O(\gamma^3), \quad [\text{B.5}]$$

where

$$\bar{\Gamma}_1 = -\frac{1}{\bar{\beta}'(1)}(1-y), \quad [\text{B.6}]$$

and

$$\bar{\Gamma}_2 = \frac{1}{[\bar{\beta}'(1)]^2} \left[ 1-y + \int_y^1 t^{-1} \ln(1-t) dt \right] - \frac{1}{2} \frac{\bar{\beta}''(1)}{[\bar{\beta}'(1)]^3} (1-y)^2, \quad [\text{B.7}]$$

with  $\bar{\beta}' = d\bar{\beta}/d\bar{\Gamma}$  and  $\bar{\beta}'' = d^2\bar{\beta}/d\bar{\Gamma}^2$ . Inserting this result into [6.1] gives

$$\hat{F} = \frac{1}{2} \gamma + \frac{1}{2\bar{\beta}'(1)} \gamma^2 + O(\gamma^3). \quad [\text{B.8}]$$

Equation [6.2] for the relative velocity of the drops is obtained by combining [B.2] and [B.8]. Equations [B.5] and [B.8] yield the surfactant distribution

$$\bar{\Gamma} = 1 + 2\bar{\Gamma}_1\hat{F} + 4\left(\bar{\Gamma}_2 - \frac{\bar{\Gamma}_1}{\bar{\beta}'(1)}\right)\hat{F}^2 + O(\hat{F}^3). \quad [\text{B.9}]$$

The concentration of surfactant at  $y = 0$  is obtained using  $\int_0^1 t^{-1} \ln(1-t) dt = -\pi^2/6$ .

For  $\hat{F} \approx 1$ , the extent of the clean-spot region  $y_c \approx 1$ . To the leading order in  $1 - y_c$ , Eq. [B.1] becomes

$$2\bar{U} \frac{d\bar{\Gamma}}{ds} = (1-s) \frac{d}{ds} \bar{\Gamma} \frac{d\bar{\beta}}{ds}, \quad [\text{B.10}]$$

where  $\hat{F} = 1$  was inserted, and

$$s = \frac{y - y_c}{1 - y_c}. \quad [\text{B.11}]$$

Integration of Eq. [B.10] with the boundary condition  $\bar{\Gamma} = 0$  at  $s = 0$  yields

$$2\bar{U} = (1-s) \frac{d\bar{\beta}}{ds} + \bar{\beta} - \bar{\Gamma}^{-1} \int_0^{\bar{\Gamma}} \bar{\beta}(\tilde{\Gamma}) d\tilde{\Gamma}. \quad [\text{B.12}]$$

Equation [6.3] is obtained by evaluating the result at  $s = 1$ .

An implicit expression for  $\bar{\Gamma}(s)$  is obtained by integrating [B.12] and inserting [6.3],

$$-\ln(1-s) = \int_0^{\bar{\Gamma}} \frac{\bar{\beta}'(\tilde{\Gamma})}{f(1) - f(\tilde{\Gamma})} d\tilde{\Gamma}, \quad [\text{B.13}]$$

where

$$f(\bar{\Gamma}) = \bar{\beta}(\bar{\Gamma}) - \bar{\Gamma}^{-1} \int_0^{\bar{\Gamma}} \bar{\beta}(\tilde{\Gamma}) d\tilde{\Gamma}. \quad [\text{B.14}]$$

For a linear equation of state

$$\bar{\Gamma} = 1 - (1-s)^{1/2}. \quad [\text{B.15}]$$

For ionic surfactant, the formulas in this appendix can be evaluated using [2.13], [6.5], [6.6], and [6.11].

## APPENDIX C

## ACKNOWLEDGMENTS

## External Force Fluctuations in Long-Time Regime

If the long-time force balance [4.5] is perturbed by a force fluctuation  $\delta\hat{F}$ , the system evolves on the short-time scale. Thus,  $\bar{U} \gg 1$  and the term involving  $I_2$  in Eq. [A.1] is unimportant. Dividing [A.1] by [3.8] yields

$$-\epsilon \frac{d\hat{F}_M}{d\epsilon} = I_1, \quad [\text{C.1}]$$

which implies Eq. [6.8] because the gap evolves on the short-time scale until  $\delta\hat{F}_M = \delta\hat{F}$ , where  $\delta\hat{F}_M$  is the perturbation of the Marangoni force.

Equation [6.9] is obtained by inserting [B.5] and [B.6] into [A.2] and using [B.8] to eliminate  $\gamma$ .

The change of variables [B.11] in Eq. [A.2] gives

$$I_1 = (1 - y_c) \int_0^1 (1 - s) \frac{\partial \bar{\beta}}{\partial s} ds \quad [\text{C.2}]$$

to leading order in  $1 - y_c$ . Transforming back to the  $y$  variable and using [6.1] yields Eq. [6.10].

This work was supported by NSF Grant CTS-9624615 and NASA Grant NAG3-1935.

## REFERENCES

1. Edwards, D. A., Brenner, H., and Wasan, D. T., "Interfacial Transport Processes and Rheology." Butterworth-Heinemann, Boston, 1991.
2. Kim, S., and Karrila, S. J., "Microhydrodynamics: Principles and Selected Applications." Butterworth-Heinemann, London, 1991.
3. Levich, V. G., "Physicochemical Hydrodynamics." Prentice-Hall, Englewood Cliffs, NJ, 1962.
4. Bławdziewicz, J., Wajnryb, E., and Loewenberg, M., *J. Fluid Mech.*, Submitted for publication.
5. Cristini, V., Bławdziewicz, J., and Loewenberg, M., *J. Fluid Mech.* **366**, 259 (1998).
6. Evans, D. F., and Wennerström, H., "The Colloidal Domain: Where Physics, Chemistry, Biology, and Technology Meet." VCH, New York, 1994.
7. Gouy, G., *J. Phys. (Paris)* **9**, 457 (1910).
8. Chapman, D. L., *Philos. Mag.* **25**, 475 (1913).
9. Augousti, A. T., and Rickayzen, G., *J. Chem. Soc. Faraday Trans. 2* **80**, 141 (1984).
10. Diaz-Herra, E., and Forstmann, F., *J. Chem. Phys.* **102**, 9005 (1995).
11. Biben, T., Hansen, J. P., and Rosenfeld, Y., *Phys. Rev. E* **57**, R3727 (1998).
12. Zinchenko, A. Z., *Prikl. Matem. Mekhan.* **46**, 72 (1982).